JOURNAL OF PROPULSION AND POWER
Vol. 9, No. 2, March–April 1993

Electrostatic Field Effects on a Rotating Liquid Film Conical Radiator

Hyo Kim,* S. G. Bankoff,† and Michael J. Miksis‡
Northwestern University, Evanston, Illinois 60208

We present a study of the interaction of an electrostatic field with a thin liquid film with a free surface flowing down the inner wall of a rotating conical radiator due to centrifugal force. First, we examine the effect of the electric field on the stability of the film flow. Next, several limits of the equations of motion are investigated analytically, and then compared with an explicit numerical calculation of the equations of motion. Also, we discuss applications of these calculations to a proposed electrostatic liquid film space radiator.

Nomenclature

a = $\bar{a}/L$
$\hat{a}$ = inlet to cone is located at $\hat{z} = -\hat{a}$
$\bar{a}$ = $\hat{a}/\cos(\beta)$
B = $\xi \cot(\beta)$
b = $\bar{b}/L$
$\hat{b}$ = outlet to cone at $\hat{z} = \hat{b}$
$\bar{b}$ = $\hat{b}/\cos(\beta)$
Ca = $2\mu U_0/\sigma$, capillary number
c = speed of light
d = characteristic film thickness
$\boldsymbol{E}$ = $[\zeta(\partial\phi/\partial x), H(\partial\phi/\partial y)]$
$\hat{E}^v$ = electric field vector in the vacuum
$\hat{E}^v_n$ = normal component of electric field
$\hat{E}^v_t$ = tangential component of the electric field
F = characteristic unit of electric field
Fr = $U_0/\sqrt{\Omega^2 \hat{R}_0 d}$, Froude number
H = $\hat{H}/d$
$\hat{H}$ = distance from wall to charged conical ring
h = $\bar{h}/\xi L$
$\hat{h}$ = fluid interface in $(\hat{r}, \hat{z})$ coordinates
$\bar{h}$ = film thickness in the transformed rectangular coordinate system
h_c = critical height
K = $\varepsilon_0 dF^2/16\pi\mu U_0$
$\bar{K}$ = K/ξ
k = wave number
k_c = critical wave number
L = characteristic length scale parallel to the wall
l = length of charged conical ring
p = $\{\hat{p} + [\sigma \cos\beta/(\hat{R}_0 + \hat{x}\sin\beta - \hat{y}\cos\beta)]\}/\rho U_0^2$
$\hat{p}$ = pressure
q = local flow rate
R = ξRe
$\hat{R}_0$ = radius of the truncated cone at $\hat{z} = -\hat{a}$
R_0 = $\hat{R}_0/L$
Re = $\rho U_0 d/\mu$, Reynolds number
$\hat{r}$ = radial distance coordinate from center of cone
$\boldsymbol{r}$ = position vector, $(\hat{r}, \hat{z})$
T = characteristic unit of time
t = $\hat{t}U_0/L$
$\hat{t}$ = time
$\bar{t}$ = ξt
U_0 = characteristic unit of velocity in the $\hat{x}$ direction
$\bar{V}$ = V/ξ
$\hat{V}$ = fluid velocity vector
V_f = fluid region
$\hat{V}_r, \hat{V}_x, \hat{V}_y, \hat{V}_z$ = velocity component in the $\hat{r}, \hat{x}, \hat{y}, \hat{z}$ directions
V_v = vacuum region
V_x = $\hat{V}_x/U_0$
V_y = $\hat{V}_y/\xi U_0$
x = $\hat{x}/L$
$\hat{x}$ = distance coordinate along the conical wall
y = $\hat{y}/\xi L$
$\hat{y}$ = distance coordinate normal to the wall
$\hat{z}$ = axial distance coordinate from the entrance of the cone
α = wave number of a disturbance
β = angle of conical wall with axis of rotation
ε_f = dielectric constant of the fluid
ε_0 = dielectric constant of the vacuum
ζ = $\hat{H}/L$
η = perturbation of h from the uniform height
μ = fluid viscosity
μ_0 = magnetic permeability
ξ = d/L
ρ = fluid density
σ = surface tension
Φ = dimensionless electric potential along $\hat{y} = H$
ϕ = $\hat{\phi}/F\hat{H}$
$\hat{\phi}$ = electric potential
$\hat{\phi}_f$ = electric potential in the fluid
$\hat{\phi}_v$ = electric potential in the vacuum
Ω = angular velocity of cone
ω = complex frequency, $\omega_r + i\omega_i$

Received April 27, 1992; revision received Aug. 24, 1992; accepted for publication Nov. 9, 1992.

*Graduate Student, Department of Chemical Engineering; currently Korea Gas Corp. R & D Training Center, 277-1 Il-dong, Ansan, Kyongki-do, 425-150, Republic of Korea.
†Walter P. Murphy Professor, Department of Chemical Engineering.
‡Associate Professor, Department of Engineering Sciences and Applied Mathematics.

I. Introduction

THE interaction of an electrostatic field with a thin liquid film flowing down the thin inner wall of a rotating conical membrane at a constant angular velocity is investigated here. The main application is the design of a very lightweight elec-

trostatic liquid film space radiator (ELFR) whose weight is expected to be in the range of 2–3 kg/m^2. This technique was proposed by Kim et al.[1] as a substitute for present-day space radiator designs which employ rather heavy armored heat pipes that can weigh more than 10 kg/m^2. Even the advanced carbon-carbon designs are expected to weigh more than 6.5 kg/m^2. The idea is to apply the electrostatic field at a position where a puncture (say from a micrometeorite) occurs in the surface of the radiator in order to prevent leakage of the liquid-metal coolant out of the puncture. Because of the internal pressure of the heat pipes, punctures by most micrometeorites and space debris can be expected to cause leakage of the coolant. The ELFR internal pressure is 0.1–1.0 Pa, so that nearly all leakage will be stopped by capillary forces. However, over a multiyear life, some large punctures can be expected. It is proposed in these cases to stop the leakage by applying an internal electrostatic field. The result is that in addition to the large weight savings, the radiator will be more reliable (for a long mission within an uncertain meteorite environment) than heat pipes, which rely on redundancy to handle loss due to punctures. Several design concepts for the ELFR can be envisioned.[1,3,4] Here we concentrate on the dynamics of the thin liquid film associated with a particular design, which is a rotating conical radiator. A similar study was performed for a liquid film flowing down an inclined plane wall in the presence of a graviety field by Kim et al.[5]

We will consider several limits of the physical parameters in order to understand the basic effect of the electrostatic field on the film flow, and to establish the feasible working ranges of the ELFR. This will be done by solving, both analytically and numerically, models for the film motion in the presence of an electric field. Several different limits of the equations of motion are also considered, and we will discuss the implications of each limiting case. This allows us clearly to identify simple solutions of the equations of motion, which give us insight into the dynamics of the film.

II. Formulation

Here we begin our investigation of the effects of the electrostatic field on a liquid film as it flows along the inner wall of a rotating conical membrane. The liquid is incompressible and viscous. The film is assumed to be thin compared to the radius of curvature of the wetted wall. The conical wall makes an angle β with the axis of rotation (see Fig. 1).

With respect to a uniformly rotating coordinate system, the dynamical equations in the absence of a gravitational body force are

$$\nabla\cdot\hat{V} = 0 \tag{1}$$

$$\frac{\partial\hat{V}}{\partial\hat{t}} + (\hat{V}\cdot\nabla)\hat{V} = -\frac{1}{\rho}\nabla\hat{p} + \frac{\mu}{\rho}\Delta\hat{V} - 2\Omega\times\hat{V} - \Omega\times(\Omega\times r) \tag{2}$$

where $\hat{V}$ is the particle velocity measured in a coordinate system rotating with a constant Ω. The liquid region is defined by $\hat{h}(\hat{t},\hat{z}) \le \hat{r} \le \hat{R}_0 + \hat{z}\tan\beta$ and $-\hat{a} \le \hat{z} \le \hat{b}$, as shown in Fig. 1.

The boundary conditions are no-slip along the wall, while along the free surface at $\hat{r} = \hat{h}(\hat{t},\hat{z})$ we have the kinematic condition, zero tangential stress condition, as well as the normal stress condition (see e.g., Landau et al.[6])

$$\sigma\left\{\frac{1}{\hat{r}}\left[1+\left(\frac{\partial\hat{h}}{\partial\hat{z}}\right)^2\right]^{-1/2} - \frac{\partial^2\hat{h}}{\partial\hat{z}^2}\left[1+\left(\frac{\partial\hat{h}}{\partial\hat{z}}\right)^2\right]^{-3/2}\right\}$$
$$= -\hat{p} + \frac{\varepsilon_0}{8\pi}\left(\frac{1}{\varepsilon_f}-1\right)[(\hat{E}_n^v)^2 + \varepsilon_f(\hat{E}_t^v)^2]$$
$$+ 2\mu\left[\left(\frac{\partial\hat{h}}{\partial\hat{z}}\right)^2\frac{\partial\hat{V}_z}{\partial\hat{z}} + \frac{\partial\hat{V}_r}{\partial\hat{r}} - \frac{\partial\hat{h}}{\partial\hat{z}}\left(\frac{\partial\hat{V}_r}{\partial\hat{z}} + \frac{\partial\hat{V}_z}{\partial\hat{r}}\right)\right]$$
$$\cdot\left[1+\left(\frac{\partial\hat{h}}{\partial\hat{z}}\right)^2\right]^{-1} \tag{3}$$

Introduce a rectangular coordinate system $(\hat{x},\hat{y})$ as shown in Fig. 1. This transformed coordinate system is defined as

$$\hat{r} = \hat{R}_0 + \hat{x}\sin\beta - \hat{y}\cos\beta$$
$$\hat{z} = \hat{x}\cos\beta + \hat{y}\sin\beta \tag{4}$$

The velocity components $(\hat{V}_r, \hat{V}_z)$ are related to the velocity components $(\hat{V}_x, \hat{V}_y)$ in the transformed system by the relations

$$\hat{V}_r = \hat{V}_x\sin\beta - \hat{V}_y\cos\beta$$
$$\hat{V}_z = \hat{V}_x\cos\beta + \hat{V}_y\sin\beta \tag{5}$$

The free surface of the film $\hat{r} = \hat{h}(\hat{t},\hat{z})$ in the axisymmetric coordinate system can be changed to

$$\hat{h}(\hat{t},\hat{z}) = \hat{R}_0 + \hat{x}\sin\beta - \bar{h}(\hat{t},\hat{x})\cos\beta \tag{6}$$

where $\hat{h}(\hat{t},\hat{x})$ is the film thickness in the transformed rectangular coordinate system. In the transformed coordinate system the liquid domain is defined by $-\bar{a} \le \hat{x} \le \bar{b}$ and $0 \le \hat{y} \le \bar{h}(\hat{t},\hat{x})$.

Above the liquid film there is a vacuum. Within the vacuum region at $\hat{H}$ from the wall is l, which is parallel to the $\hat{x}$ axis and symmetric about the $\hat{z}$ axis. Let $\hat{x} = 0$ be at the center of the charged ring along the $\hat{x}$ axis. Suppose that we define d as the characteristic thickness of the film and

$$\xi = (d/L) \tag{7}$$

If we assume that $\xi \ll 1$, we have a film which is thin, relative to the expected length scale of the disturbances. If $d/\hat{H} \ll 1$, the charged foil is very far from the wall relative to the thickness of the film. To leading order in $d/\hat{H}$, we can then assume that the charged ring does not see the film, and the electrostatic problem for the electric field decouples from the fluid dynamics problem. The ratio $\zeta = \hat{H}/L$ is assumed to be order one.

We will assume throughout that $L/\hat{R}_0$ is order one. Hence, the thin axisymmetric film is locally two-dimensional. We will

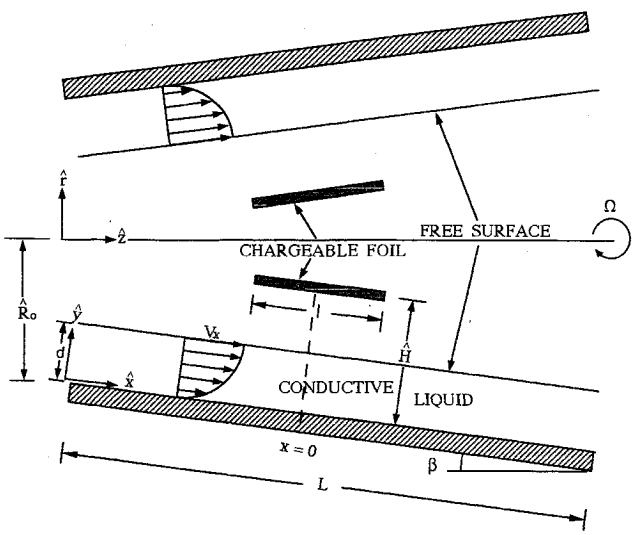

Fig. 1 Coordinate scheme of the rotating flow with $x = 0$ as puncture location.

also assume that the finite-sized charged foil is very far from the fluid inlet and outlet points. Together, these assumptions allow us to approximate the electric field due to the charged foil by that resulting from a two-dimensional finite charged foil above an infinite plane, i.e., we assume that field decays to zero as the magnitude of $\hat{x}$ gets large. Thus, we can consider this geometry as in the plane flow case, and the electric field is determined by solving the Laplace equation

$$\nabla^2\hat{\phi} = 0 \tag{8}$$

for the electric potential $\hat{\phi}(\hat{x}, \hat{y})$ in the fluid, $\hat{\phi}_f$, and for the electric potential, $\hat{\phi}_v$, in the vacuum region above the fluid but below the charged foil. V_f is defined by $0 \le \hat{y} \le \bar{h}(\hat{x}, \hat{t})$ and $-\bar{a} \le \hat{x} \le \bar{b}$ (later we will assume that $\bar{a}$ and $\bar{b}$ tend to infinity), where $\hat{y} = \bar{h}(\hat{x}, \hat{t})$ is the height of the film above the inclined wall, V_v is defined by the strip $-\bar{a} \le \hat{x} \le \bar{b}$ and $\bar{h}(\hat{x}, \hat{t}) \le \hat{y} \le \hat{H}$. We will use the subscript or superscript f for quantities in V_f, and the subscript or superscript v for quantities in V_v, unless no confusion can occur. The boundary conditions are that

$$\hat{\phi}(\hat{x}, \hat{H}) = F\hat{H}\Phi(\hat{x}), \quad \text{for} \quad \hat{y} = \hat{H}$$

$$\hat{\phi} = 0, \quad \text{for} \quad \hat{y} = 0 \tag{9}$$

The function $\Phi(\hat{x})$ is a given dimensionless function of $\hat{x}$, and the product $F\hat{H}$ is a constant with the units of electric potential. Along $\hat{y} = \bar{h}(\hat{x}, \hat{t})$ we have the boundary conditions that the tangential electric field and the normal displacement field are continuous

$$\hat{\phi}^f(\hat{x}, \bar{h}, \hat{t}) = \hat{\phi}^v(\hat{x}, \bar{h}, \hat{t}), \quad \varepsilon_f \frac{\partial\hat{\phi}^f}{\partial n} = \varepsilon_0 \frac{\partial\hat{\phi}^v}{\partial n} \tag{10}$$

Here the partial derivative is in the direction of the outward unit normal n to the interface.

The liquid film is governed by the incompressible Navier-Stokes equations. Letting d be the unit of length in the $\hat{y}$ direction, L the unit of length in the $\hat{x}$ direction, U_0 the unit of velocity in the $\hat{x}$ direction, ξU_0 the unit of velocity in the $\hat{y}$ direction, L/U_0 the unit of time, ρU_0^2 the unit of pressure, F the unit of electric field, and ε_0 the unit of the dielectric constant, we can determine the dimensionless equations of motion. The continuity equation becomes

$$\frac{\partial V_x}{\partial x} + \frac{\partial V_y}{\partial y} + \frac{V_x \sin\beta - \xi V_y \cos\beta}{R_0 + x\sin\beta - \xi y\cos\beta} = 0 \tag{11}$$

while the x and y components of the momentum equation are

$$\frac{\partial V_x}{\partial t} + V_x\frac{\partial V_x}{\partial x} + V_y\frac{\partial V_x}{\partial y} = -\frac{\partial p}{\partial x}$$

$$- \frac{2}{Re}\frac{\xi}{Ca}\frac{\sin\beta\cos\beta}{(R_0 + x\sin\beta - \xi y\cos\beta)^2} + \frac{\xi}{Re}$$

$$\cdot\left[\frac{\partial^2 V_x}{\partial x^2} + \frac{1}{\xi^2}\frac{\partial^2 V_x}{\partial y^2} - \frac{V_x\sin^2\beta - \xi V_y\sin\beta\cos\beta}{(R_0 + x\sin\beta - \xi y\cos\beta)^2}\right.$$

$$\left. + \frac{\sin\beta\dfrac{\partial V_x}{\partial\hat{x}} - \dfrac{\cos\beta}{\xi}\dfrac{\partial V_x}{\partial y}}{R_0 + x\sin\beta - \xi y\cos\beta}\right] + \frac{1}{Fr^2}\frac{\sin\beta}{\xi}$$

$$\cdot\left(1 + \frac{x}{R_0}\sin\beta - \xi\frac{y}{R_0}\cos\beta\right) \tag{12}$$

$$\xi\left(\frac{\partial V_y}{\partial t} + V_x\frac{\partial V_y}{\partial x} + V_y\frac{\partial V_y}{\partial y}\right) = -\frac{1}{\xi}\frac{\partial p}{\partial y}$$

$$+ \frac{2}{Re}\frac{\xi}{Ca}\frac{\cos^2\beta}{(R_0 + x\sin\beta - \xi y\cos\beta)^2} + \frac{\xi}{Re}$$

$$\cdot\left[\xi\frac{\partial^2 V_y}{\partial x^2} + \frac{1}{\xi}\frac{\partial^2 V_y}{\partial y^2} + \frac{V_x\sin\beta\cos\beta - \xi V_y\cos^2\beta}{(R_0 + x\sin\beta - \xi y\cos\beta)^2}\right.$$

$$\left. + \frac{\xi\sin\beta\dfrac{\partial V_y}{\partial x} - \cos\beta\dfrac{\partial V_y}{\partial y}}{R_0 + x\sin\beta - \xi y\cos\beta}\right] - \frac{1}{Fr^2}\frac{\cos\beta}{\xi}$$

$$\cdot\left(1 + \frac{x}{R_0}\sin\beta - \xi\frac{y}{R_0}\cos\beta\right) \tag{13}$$

The boundary conditions must still be given. Along the solid wall, $y = 0$, we have the no-slip boundary condition

$$V_x = V_y = 0 \tag{14}$$

On the fluid interface, $y = h(x, t)$, we have the kinematic condition

$$\frac{\partial h}{\partial t} + V_x\frac{\partial h}{\partial x} = V_y \tag{15}$$

the continuity of tangential stress

$$\left[1 - \xi^2\left(\frac{\partial h}{\partial x}\right)^2\right]\left(\frac{\partial V_x}{\partial y} + \xi^2\frac{\partial V_y}{\partial x}\right)$$

$$+ 2\xi^2\frac{\partial h}{\partial x}\left(\frac{\partial V_y}{\partial y} - \frac{\partial V_x}{\partial x}\right) = 0 \tag{16}$$

and the continuity of normal stress

$$\frac{\xi^2}{Ca}\left(\frac{\partial^2 h}{\partial x^2}\left[1 + \xi^2\left(\frac{\partial h}{\partial x}\right)^2\right]^{-3/2}\right.$$

$$+ \frac{\sin\beta}{R_0 + x\sin\beta - \xi y\cos\beta}\frac{\partial h}{\partial x}\left[1 + \xi^2\left(\frac{\partial h}{\partial x}\right)^2\right]^{-1/2}$$

$$\left. + \frac{1}{\xi}\frac{\cos\beta}{R_0 + x\sin\beta - \xi y\cos\beta}\left\{\left[1 + \xi^2\left(\frac{\partial h}{\partial x}\right)^2\right]^{-1/2} - 1\right\}\right) = -\frac{Re}{2}p + K\left(\frac{1}{\varepsilon_f} - 1\right)[(E_n^v)^2 + \varepsilon_f(E_t^v)^2]$$

$$+ \xi\left[\xi^2\left(\frac{\partial h}{\partial x}\right)^2\frac{\partial V_x}{\partial x} - \frac{\partial h}{\partial x}\left(\frac{\partial V_x}{\partial y} + \xi^2\frac{\partial V_y}{\partial x}\right) + \frac{\partial V_y}{\partial y}\right]$$

$$\cdot\left[1 + \xi^2\left(\frac{\partial h}{\partial x}\right)^2\right]^{-1} \tag{17}$$

Here we have set the pressure in the vacuum above the liquid film to zero. Also we define the dimensionless electric field as

$$\boldsymbol{E} = \left(\zeta\frac{\partial\phi}{\partial x}, \quad H\frac{\partial\phi}{\partial y}\right) \tag{18}$$

with the normal component defined as $E_n = \boldsymbol{E}\cdot n$ and the tangential component defined as $E_t = \boldsymbol{E}\cdot\tau$, where τ is the

unit tangent to the interface. We see from Eq. (17) that the charged foil suspended above the liquid film only influences the fluid motion by way of the inhomogeneous term in the normal stress equation.

The dimensionless constants, Re, Ca, Fr, and K all need to be specified. Suppose we consider a specific fluid in a given experimental situation where the only free parameter is the characteristic velocity U_0. Then Re, Fr, and Ca vary linearly with U_0, while K is inversely proportional to U_0. For our calculations we will take the physical parameters for lithium at 700 K ($\mu = 0.0038p$, $\sigma = 363.2$ dyne/cm, and $\rho = 0.493$ g/cm^3). For fixed electric field strength F, K varies as the Reynolds number changes.

Equations (11–17) determine the motion of the liquid film. Initial conditions are still required to solve for the evolution of the liquid. In addition, there should be an inlet boundary condition to solve this problem. The entrance length is assumed to be very short and the flow quickly has a parabolic velocity profile.

III. Linear Stability

Linear stability for liquid film flow down an inclined plane was studied by Benjamin[7] and Yih.[8] In the long-wave limit their result is that the liquid is stable if

$$Re < \tfrac{5}{6}\cot(\beta) \tag{19}$$

Our aim here is to generalize this result to include the effect of the electric field in the rotating system. Assume that the entrance radius R_0 is very large, i.e., $R_0 >> 1$. Then from Eqs. (11–13) the leading-order mass and momentum equations reduce to the equations of film flow down an inclined plane,[5] and can be used to determine the local stability. In the long-wave limit, i.e., $a \to 0$ where $a \geq 0$ is the wave number of the disturbance, with the same analysis as in Kim et al.,[5] one can show that the uniform flow is stable if

$$Re < \tfrac{5}{6}\cot(\beta) - \tfrac{10}{9}\,\mathrm{KW} \tag{20}$$

where in the long wave limit

$$W \to \frac{H^2[1 - (1/\varepsilon_f)]^2}{[(1/\varepsilon_f) + H - 1]^3} \tag{21}$$

For $\varepsilon_f > 1$, the effect of the electric field is to lower the value of the critical Reynolds number for linear stability. The unit of d is also assumed to be constant, although d decreases as x increases in the real conical flow. Thus, the most unstable situation occurs at the inlet boundary where the Reynolds number has the largest value. In order to understand the effect of the electric field on the stability for larger wave numbers we solve the resulting linear eigenvalue problem, i.e., a modified Orr-Sommerfeld equation, numerically. The characteristic unit of velocity U_0 is defined as $\rho\Omega^2 R_0 d^2 \sin\beta/3\mu$.

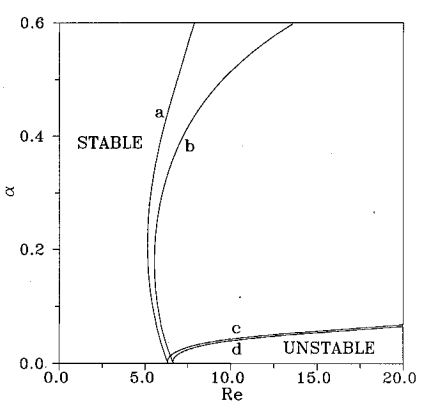

Fig. 2 Neutral stability curves in the $\alpha - Re$ plane for $\beta = 0.1$ rad, $H = 13\frac{1}{3}$: a) $K = 110$ and $Ca = \infty$, b) $K = 0$ and $Ca = \infty$, c) $K = 110$ and $Ca = 5.4 \times 10^{-5}$, and d) $K = 0$ and $Ca = 5.4 \times 10^{-5}$.

The resulting eigenvalue problem can be solved numerically by using a shooting method.[2,5] We consider a perfectly conducting fluid, i.e., $\varepsilon_f = \infty$. In Fig. 2 we set $\beta = 0.1$ rad, $H = 10$, and solve the eigenvalue problem. In Fig. 2 we sketch the neutral stability curves (i.e., $c_i = 0$) in the $a - Re$ plane for the case of $Ca = \infty$, i.e., no surface tension, and for $Ca = 5.4 \times 10^{-5}$. Also in Fig. 2 we sketch the neutral stability curves for both $K = 0$, (no electric field) and $K = 110$. We see that small Reynolds number flows are stable, while increasing Re for fixed a will cause the flow to become unstable. Note that the effect of the electric field is to lower the value of the critical Reynolds number at which the flow becomes unstable. The critical Reynolds number decreases with increasing β and decreasing surface tension, similarly to the results of Benjamin[7] and Yih.[8]

IV. Thin-Film Limit

We consider the thin-film limit, $\xi << 1$, of Eqs. (8–17) and derive a nonlinear evolution equation for the height, $h(x, t)$ of the film. The film thickness is set to $h = 1$ at $x = -a$ for the inlet boundary condition.

A. Order-One Reynolds Numbers

Steady-State Solutions at Leading Order in ξ

Here, we will determine the steady-state solution at leading order in ξ for order-one Reynolds numbers. A similar analysis for a thin film flowing down an inclined plane, but without an electric field has been performed by Benney[10] and Gjevik,[11] and with an electric field by Kim et al.[5] The steady-state solution of Eqs. (11–17) is expressed as a perturbation expansion in ξ, e.g.

$$h(t, x) = h_0(x) + \xi h_1(t, x) + \cdots \tag{22}$$

On substituting these expansions into Eqs. (11–17), we can obtain the leading-order equations of motion (assuming ξ^2/Ca is order one). From the leading-order equations we determine that the leading-order film thickness at steady state is

$$h_0 = \left(\frac{R_0 - a\sin\beta}{R_0 + x\sin\beta}\right)^{2/3} \tag{23}$$

where the inlet boundary condition $h_0 = 1$ at $x = -a$ is used. The leading-order pressure is

$$p_0 = -\frac{2\xi^2}{ReCa}\left(\frac{\partial^2 h_0}{\partial x^2} + \frac{\sin\beta}{R_0 + x\sin\beta}\frac{\partial h_0}{\partial x}\right) - \frac{\cos\beta}{Fr^2} \cdot\left(1 + \frac{x}{R_0}\sin\beta\right)(y - h_0) + \frac{2K}{Re}\left(\frac{1}{\varepsilon_f} - 1\right) \cdot[(E_n^v)^2 + \varepsilon_f(E_t^v)^2] \tag{24}$$

We see from Eq. (23) that the leading-order film height h_0 continuously decreases from $h_0 = 1$ as x increases and it is not affected by the electric field. This occurs because there is no leading-order pressure gradient in the leading order x direction momentum equation. The leading-order pressure p_0 depends on the strength of the electric field. The design of ELFR requires a negative pressure under the charged foil, which would stop a leak out of a puncture. For this purpose we can calculate a critical film thickness h_{0c} from Eq. (24) for the negative pressure on the wall at $y = 0$

$$h_{0c} = \frac{2K}{Re}\frac{Fr^2}{\cos\beta}\frac{(E_n^v)^2}{[1 + (x/R_0)\sin\beta]} \tag{25}$$

Here we neglect the surface tension of the fluid ($Ca \to \infty$) and assume the fluid has perfect conductivity ($\varepsilon_f \to \infty$). To get a negative pressure on the radiator wall, h_0 should be less than h_{0c} in this analysis.

Solutions on a Long-Time Scale

Suppose we only look for solutions which vary on a long time scale, i.e., $t = O(1/\xi)$, and assume that the velocity components V_x and V_y are order ξ. In this limit our results will be similar to the two-dimensional case of a thin film flowing down an inclined plane, with the centrifugal body force replacing the gravitational force.

Two limits involving the placement of the charged foil will be discussed here. In the first we assume that the electric potential along $y = H$ depends on the slow x scale, and that the characteristic length scale in the y direction in the vacuum region is d. In the second limit we assume that the characteristic length scale in the vertical direction is L, and therefore, the thin film is not seen at leading order in ξ by the charged foil. In the first of these limiting cases we find from the dimensionless version of Eqs. (8–10) that at leading order in ξ, the electric potential is a linear function of y, with coefficients which depend on the slow scale x and t. Using the boundary conditions [Eqs. (9) and (10)] this implies that

$$\phi_0^f = \Phi(x)(y/\varepsilon_f)\{h(x,t)[(1/\varepsilon_f) - 1] + H\}^{-1}$$

$$\text{for} \quad 0 < y < h(x,t) \tag{26}$$

$$\phi_0^v = \Phi(x)\big(1 + (y - H)\{h(x,t)[(1/\varepsilon_f) - 1] + H\}^{-1}\big)$$

$$\text{for} \quad h(x,t) < y < H \tag{27}$$

Here we have set the boundaries $x = a$ and b to infinity. Additional corrections to the electric potential require the next order correction in $h(x, t)$. The second of the limiting cases will be discussed below. In the following we will see that as long as $\bar{K}$ is assumed to be order one, then we only need the leading order behavior of ϕ in order to determine h to two orders in ξ.

The long-time scale solutions will be determined in two steps. First, let $V_x = \xi\bar{V}_x$, $V_y = \xi\bar{V}_y$, $t = \bar{t}/\xi$, $K = \xi\bar{K}$, $\beta = O(\xi)$, $U_0 = \rho\Omega^2 R_0 d^2/3\mu$, in Eqs. (11–17), and retain only terms up to order ξ. Second, note that the scaled continuity equation allows the use of a stream function Ψ, in terms of which $\bar{V}_x$ and $\bar{V}_y$ can be expressed as $\bar{V}_x = (R_0 + x\sin\beta - \xi y\cos\beta)^{-1}(\partial\Psi/\partial y)$, and $\bar{V}_y = -(R_0 + x\sin\beta - \xi y\cos\beta)^{-1}(\partial\Psi/\partial x)$. Expanding Ψ in a power series in ξ and substituting back into the equations resulting from the first part, and then solving the equations for the first two orders in ξ, we can determine an equation for $h(t, x)$ accurate to $O(\xi^2)$ (see Kim[12] for details). The result of these calculations is

$$\frac{\partial h}{\partial \bar{t}} + \frac{\partial}{\partial x}\left[h^3\left(\frac{\sin\beta}{\xi} - \cos\beta\frac{\partial h}{\partial x}\right)\right] + \frac{2}{3}\frac{\partial}{\partial x}$$

$$\cdot\left(h^3\left\{\xi\bar{K}\left(1 - \frac{1}{\varepsilon_f}\right)\frac{\partial}{\partial x}(E_{0n}^v)^2 + \frac{\xi^2}{Ca}\left[\frac{\partial^3 h}{\partial x^3} - \frac{\cos\beta}{R_0}\frac{\partial h}{\partial x}\right.\right.\right.$$

$$- \frac{\cos\beta}{R_0^2}\frac{\sin\beta}{\xi} - \frac{1}{3}\frac{\sin\beta}{R_0^2}\cos\beta - \frac{1}{2}\frac{\sin\beta}{R_0^3}\cos^2\beta$$

$$\left.\left.\left.\cdot\left(4\frac{\partial h}{\partial x} + 5h\right) + \frac{\xi}{R_0^3}\cos^4\beta h\frac{\partial h}{\partial x} + \frac{3}{4}\frac{\xi}{R_0}\cos\beta h\frac{\partial^3 h}{\partial x^3}\right]\right.\right.$$

$$\left.\left. + \frac{3}{R_0}\frac{\sin^2\beta}{\xi}x + \frac{3}{8}\frac{\xi}{R_0}\cos^2\beta h\frac{\partial^2 h}{\partial x^2}\right\}\right) + \frac{h^2}{R_0}\frac{\partial h}{\partial x}$$

$$\cdot\left(\xi\cos^2\beta h\frac{\partial h}{\partial x} - 3\frac{\sin^2\beta}{\xi}x\right) - \frac{h^2}{R_0}\cos\beta\sin\beta$$

$$\cdot\left[4h\frac{\partial h}{\partial x} + 3x\left(\frac{\partial h}{\partial x}\right)^2 + xh\frac{\partial^2 h}{\partial x^2}\right] - \frac{2}{3}\frac{\xi^2}{Ca}\frac{h^3}{R_0^2}$$

$$\cdot\left[2\cos^2\beta\left(\frac{\partial h}{\partial x}\right)^2 + \xi R_0\cos\beta\frac{\partial h}{\partial x}\frac{\partial^3 h}{\partial x^3} + \frac{3}{4}\cos^2\beta h\frac{\partial^2 h}{\partial x^2}\right]$$

$$+ 2\frac{\xi^2}{Ca}\frac{h^2}{R_0}\left[\sin\beta\frac{\partial h}{\partial x}\frac{\partial^2 h}{\partial x^2} - \xi\cos\beta\left(\frac{\partial h}{\partial x}\right)^2\frac{\partial^2 h}{\partial x^2}\right.$$

$$+ \frac{1}{3}\xi\cos\beta h\left(\frac{\partial^2 h}{\partial x^2}\right)^2 + \frac{2}{3}\sin\beta h\frac{\partial^3 h}{\partial x^3}$$

$$\left. - \frac{1}{3}\frac{\cos\beta}{R_0^2}\frac{\sin^2\beta}{\xi}h\right] = 0 \tag{28}$$

Here $E_{0n}^v = H(\partial\phi_0^v)/\partial y$ on $y = h$ represents the leading order contribution of the electric field on the thin film. We see from Eq. (28) that for $\bar{K}$ order one we only need the leading-order correction to the normal electric field in order to determine the h to second order in ξ. The effect of the electric field occurs in this approximation only at order ξ. The value of the partial derivative of ϕ_0^v can be determined from Eq. (27). In Eq. (28) we have assumed that the coefficient ξ^2/Ca is order one.

Suppose that $H >> 1$, i.e., the conducting plate is far from the inclined wall. In this limit we find that $E_{0n}^v = \Phi(x)$. Hence, the effect of the electric field in Eq. (28) is just the derivative of a given function of x times h^3. Changes in the potential along the conducting plate are felt explicitly in this limit, but without accounting for the effect of variations of h on the electric field. This implies that we should be able to generalize this limit to the case where the characteristic length scale in the vertical for the determination of the electric field is of order L. This will be done shortly.

Now suppose that H is finite. Then we find that the denominator of the term containing K becomes large as h approaches $H/(1 - 1/\varepsilon_f)$. This implies that since $H/(1 - 1/\varepsilon_f) > H$, the approximation breaks down and a shock could possibly form. Additional work needs to be done to show if and when this can occur.

Suppose we keep only the leading order in ξ terms of Eq. (28). For simplicity, assume that the fluid is a perfect conductor, i.e., $\varepsilon_f \to \infty$. Clearly, only the first two terms in Eq. (28) will be included under the above assumptions. The resulting equation is a nonlinear parabolic partial-differential equation for disturbances moving toward increasing x. This result is independent of the effect of the electric field. Suppose we assume that $K = O(1)$ and determine how the electric field influences the evolution of the thin film at leading order. The result is (neglecting the capillary terms)

$$\frac{\partial h}{\partial \bar{t}} + \frac{\partial}{\partial x}\left\{h^3\left[\frac{\sin\beta}{\xi} - \cos\beta\frac{\partial h}{\partial x} + \frac{2}{3}K\frac{\partial}{\partial x}(E_{0n}^v)^2\right]\right\} = 0 \tag{29}$$

This is the same evolution equation studied in Kim et al.[5] for two-dimensional film flow down an inclined plane.

The above observations of this leading-order unsteady thin film model for $K = O(1)$ imply that film flow in the presence of a finite conducting foil can be a stable process, in that a disturbance can grow while it is under the charged foil, but once it passes, the height can stabilize. From the point of view of the ELFR, this is a positive observation since as long as

the film flow is able to pass the conducting foil in a continuous manner the ELFR is operable. Our concern would be the possibility of the fluid touching the foil or leaving the thin film limit, and hence, cooling at a rate unpredictable by this analysis.

Suppose $\Phi = 1$ (for small K) and consider linear stability analysis of Eq. (29) about $h = 1$. It is easy to show that Eq. (29) is linearly stable if $\cos\beta - \frac{4}{3}KH^2/(H-1)^3 > 0$. This result for the linear stability can be expected from Sec. III.

B. Large Reynolds Numbers

We consider the thin film limit with $Re = O(1/\xi)$, and select U_0 as the mean velocity of a flow within a rotating conical wall, i.e., $\rho\Omega^2 R_0 d^2 \sin\beta/3\mu$. Assume that $Fr^2 = O(1/\xi)$, while all the other variables are order one. Under these conditions we can derive a nonlinear system of evolution equations valid for the first two orders in ξ. Unfortunately, it is not systematically possible to solve these nonlinear equations. In order to obtain a simple evolution equation, we use the Karman-Pohlhausen approximation. This has recently been applied to other thin-film problems with considerable success.[5,13,14]

Let $R = \xi Re = O(1)$ and note that here the angle $\beta = O(1)$. Using these assumptions in Eqs. (11–17) the terms to order ξ can be determined. The result is (for $\varepsilon_f = \infty$)

$$\frac{\partial V_x}{\partial x} + \frac{\partial V_y}{\partial y} + \frac{V_x \sin\beta}{R_0 + x\sin\beta} + \xi\frac{V_x \sin\beta\cos\beta}{(R_0 + x\sin\beta)^2}y = 0 \tag{30}$$

for conservation of mass while the momentum equations become

$$\frac{\partial V_x}{\partial t} + V_x\frac{\partial V_x}{\partial x} + V_y\frac{\partial V_x}{\partial y} = -\frac{\partial p}{\partial x} + \frac{1}{R}\cdot\left[\frac{\partial^2 V_x}{\partial y^2} - \xi\cos\beta\frac{\partial V_x}{\partial y}\left(\frac{1}{R_0 + x\sin\beta}\right)\right] + \frac{1}{Fr^2}\frac{\sin\beta}{\xi}\left(1 + \frac{x}{R_0}\sin\beta - \xi\frac{y}{R_0}\cos\beta\right) \tag{31}$$

$$\frac{\partial p}{\partial y} = -\frac{\cos\beta}{Fr^2}\left(1 + \frac{x}{R_0}\sin\beta\right) \tag{32}$$

Integrating the above equations along with their boundary conditions is clearly difficult, even though they represent only the leading-order behavior of the thin film. In order to simplify the analysis, we introduce the Karman-Pohlhausen approximation

$$V_x = \frac{3q}{h}\left[\frac{y}{h} - \frac{1}{2}\left(\frac{y}{h}\right)^2\right] \tag{33}$$

where q is defined by

$$q = \int_0^h V_x\,dy \tag{34}$$

To derive the nonlinear evolution equation, one integrates Eqs. (30–32), then substitutes Eq. (33) into the horizontal momentum Eq. (31), and finally integrates Eq. (31) in y from 0 to h. Prokopiou et al.[13] give additional details. The result of these calculations is a coupled set of nonlinear hyperbolic equations for h and q

$$\frac{\partial h}{\partial t} + \frac{\partial q}{\partial x} + \frac{\sin\beta}{R_0 + x\sin\beta}q + \frac{5}{8}\xi\frac{\sin\beta\cos\beta}{(R_0 + x\sin\beta)^2}hq = 0 \tag{35}$$

$$\frac{\partial q}{\partial t} + \frac{\partial}{\partial x}\left(\frac{6}{5}\frac{q^2}{h}\right) + \frac{6}{5}\frac{\sin\beta}{R_0 + x\sin\beta}\frac{q^2}{h} + \frac{33}{40}\cdot\xi\frac{\sin\beta\cos\beta}{(R_0 + x\sin\beta)^2}q^2 = -\frac{\cos\beta}{Fr^2}h\cdot\left(\frac{\partial h}{\partial x} + \frac{1}{2}\frac{\sin\beta}{R_0}h + \frac{x}{R_0}\sin\beta\frac{\partial h}{\partial x}\right) + \xi\frac{2K}{R}\frac{\partial(E_n^v)^2}{\partial x}h - \frac{3}{R}\frac{q}{h^2} - \frac{3}{2}\frac{\cos\beta}{R}\frac{\xi}{R_0 + x\sin\beta}\frac{q}{h} + \frac{h}{Fr^2}\frac{\sin\beta}{\xi}\cdot\left(1 + \frac{x}{R_0}\sin\beta - \frac{1}{2}\frac{\xi}{R_0}\cos\beta h\right) \tag{36}$$

where

$$(Re\sin\beta/3Fr^2) = 1 \tag{37}$$

Equation (36) reduces to the two-dimensional plane flow result for $R_0 >> 1$. As in Sec. III, we consider this stability problem from a local point of view, where a leading-order steady-state solution of Eqs. (35) and (36) exists of the form $h = 1$ and $q = 1$. Again d is to be interpreted as the local thickness. Letting η represent the perturbation of h from the uniform height, i.e., $h = 1 + \eta$, and $B = \xi\cot\beta$, we can derive the linearized disturbance equation

$$\frac{\partial^2\eta}{\partial t^2} + \frac{12}{5}\frac{\partial^2\eta}{\partial t\partial x} + \left[\frac{6}{5} - \frac{3B}{R} + \frac{6\xi KH^2}{R(H-1)^3}\right]\frac{\partial^2\eta}{\partial x^2} + \frac{3}{R}\frac{\partial\eta}{\partial t} + \frac{9}{R}\frac{\partial\eta}{\partial x} = 0 \tag{38}$$

Looking for a time-harmonic solution proportional to $\exp[i(kx - \omega t)]$, where k is the real wave number and $\omega = \omega_r + i\omega_i$ is the complex frequency, we find from Eq. (38) the dispersion relation

$$\omega^2 - \frac{12}{5}k\omega + \left[\frac{6}{5} - \frac{3B}{R} + \frac{6\xi KH^2}{R(H-1)^3}\right]k^2 + i\frac{3\omega}{R} - i\frac{9k}{R} = 0 \tag{39}$$

The condition for onset can be determined from Eq. (39) by requiring that the first and second derivatives of ω_i, with respect to k, vanish exactly. The result of this calculation is that the critical values of the Reynolds number R_c, the wave number k_c, and the leading-order behavior of ω_r are given by

$$R = B - \frac{2\xi KH^2}{(H-1)^3}, \quad k_c = 0, \quad \omega_r \sim 3k \tag{40}$$

The above results without the electrostatic field have the same forms as in the case of thin film flowing down an inclined plane discussed by Prokopiou et al.[13]

It is of interest to consider the steady-state solutions of Eqs. (35) and (36) for R_0 large. In this limit, note that Eq. (35) implies $q = 1$. Then the steady-state solution determined from Eq. (36) is

$$\frac{dh}{dx}\left\{h^3\left[\frac{\cos(\beta)}{Fr^2} - \frac{4\xi KH^2}{R}\frac{\Phi^2(x)}{(H-h)^3}\right] - \frac{6}{5}\right\} = \frac{\cos(\beta)}{BFr^2}h^3 - \frac{3}{R} + \frac{4\xi KH^2}{R}\frac{h^3\Phi(x)}{(H-h)^2}\frac{d\Phi}{dx} \tag{41}$$

Here, we have used the limiting form of E_n^v as given by Eq. (27). This steady solution will have a point where there is infinite slope, a shock, when the coefficient of the first derivative term is zero. Hence, we can determine a critical height as a function of the parameters. Solving for this critical height h_c involves solving a sixth-order polynomial in h. In the limit where $H >> 1$, we find using Eq. (37) that

$$h_c = \left[\frac{6R}{5}\left(3B - \frac{4\xi K\Phi^2}{H}\right)^{-1}\right]^{1/3} \tag{42}$$

This result, but without the effect of the electric field ($K = 0$), can be also found in Rahman et al.[14] The effect of the electric field is to raise h_c for $\Phi > 0$. We note that Eq. (42) relates the Reynolds number to the critical film thickness, with h_c^3 being linearly proportional to R. As the Reynolds number decreases, the value of h_c decreases, at which we can expect a shock. Using Eq. (37) we can express this result in terms of Fr and a critical Froude number can be identified.

The steady-state solution of the Karman-Pohlhausen approximation of Eqs. (35) and (36) is shown in Fig. 3. In order to simulate a slowly varying potential, we set $\Phi = \exp(-100x^2)$ in Eq. (27) and set $E_{0n}^v = H(\partial\phi_0^v/\partial y)$. This potential has the slowly varying form of the assumptions. For boundary conditions we set $h = 1$ and $q = 1$ at a sufficient distance from the foil while the effect of the electric field is very small. In order to simulate an experimental situation, we set $\beta = 0.1$ rad, $\hat{R}_0 = 6$ cm, $\Omega = 3$ rad/s, $\xi = 0.0033$ and $F = 15$ kV/cm at $Re = 30.3$, 242.0, or $F = 18$ kV/cm at $Re = 472.6$, with the physical properties of lithium at 700 K. Then we vary the upstream depth of the film d, which varies the mean velocity U_0, and therefore, Re, K, and H. In Fig. 3 we plot the two cases of $Re = 242.0$, 472.6, which correspond to the values of $K = 22.5$, 26.0, and the values of $H = 10.0$, 8.0, respectively. The film thins with increasing Re, and the effect of the electric field is to cause a sudden decrease, then an increase, and finally a decrease of the film height under the foil. As Re decreases, the steady-state profiles can change. For example, the steady-state profile for $Re = 30.3$ (not plotted) has the film thickening and slowing down with increasing distance from the foil. These are large Reynolds numbers, but they illustrate the predictions of this theory. In particular, we find that the percent perturbation of the interface decreases as the Reynolds number increases, i.e., as d increases.

Finally, one could ask if the steady solution given by Eqs. (35) and (36) is linearly stable. This could be checked by linearizing Eqs. (35) and (36) about steady solutions in h and q. This calculation is similar in spirit to the stability analysis for Sec. III, but now the equilibrium solution is only known from a numerical integration. Also, the periodicity assumption used in Sec. III is no longer valid since we are solving the problem on a semi-infinite interval with the boundary condition, $h = 1$ and $q = 1$, given at some finite negative value of x. Hence, stability is related to the size of the interval of integration. By looking for solutions of this linear problem proportional to $\exp(ct)$ an eigenvalue problem for c can be identified. This eigenvalue problem has been solved, and only negative values of c have been determined for all ranges of the parameters we have considered. Therefore, it appears that the steady (continuous) solutions of the Karman-Pohlhausen approximation are linearly stable.

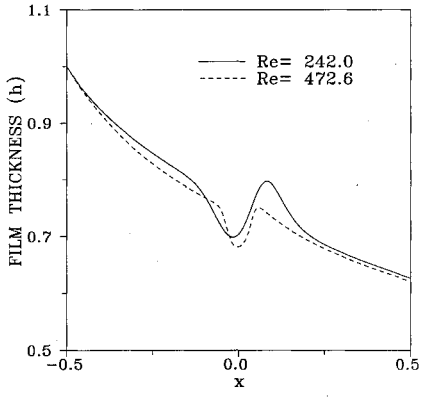

Fig. 3 Steady-state solutions of the Karman-Pohlhausen model with zero surface tension, $F = 15$ kV/cm, $\beta = 0.1$ rad and with $Re = 242.0$, 472.6.

V. Numerical Solutions

In the previous section we considered several asymptotic solutions of the system [Eqs. (8–17)]. This approach was taken because the system represents a complicated nonlinear moving boundary problem whose solution involves solving the Navier-Stokes equations coupled to the electrostatic equations. A complete numerical solution of this problem is still very difficult. Here we will consider the limit where $H >> 1$, so that the charged foil is far away from the wall of the flowing film. As noted before, this decouples the electrostatic problem from the fluids problem. Hence, if a solution of the electrostatic problem can be determined, we need only solve Eqs. (11–17), where E_n^v now represents a known forcing function. We solve this moving boundary problem for the Navier-Stokes equations by using a modification of the code SOLA.[15] SOLA uses a finite-difference technique based on the Marker-and-Cell method to solve the two-dimensional equations of motion of a fluid written in terms of Cartesian coordinates. Hence, to solve Eqs. (11–13), some additional terms must be inserted into the original version of the code, consistent with the Marker-and-Cell technique.[16] We have used this code since it is easily modified for the presence of the electric field.

Suppose that the fluid is a perfect conductor and that Φ at $y = H$ is given by

$$\Phi(x) = \begin{cases} 1 & \text{for } -l/2 \le x \le l/2 \\ 0 & \text{otherwise} \end{cases} \tag{43}$$

Here, we again assume that a and b tend to infinity, so the electrostatic problem is two-dimensional and defined on an infinite interval. The solution of this electrostatic problem can be found in Morse and Feshbach.[17] In terms of the normal component of the electric field along the wall $y = 0$ we have

$$E_n^v = -1 + \frac{1}{1 + \exp[-(\pi/\xi H)(l/2 - x)]} + \frac{1}{1 + \exp[-(\pi/\xi H)(l/2 - x)]} \tag{44}$$

Equation (44) can now be used in Eq. (17), and the resulting system can be solved numerically. We note that while we needed to have a slowly varying electric field in order for our thin film analysis to be valid, this assumption is not necessary here since we will solve the complete Navier-Stokes equations. The only requirements for the validity of this calculation is that $H >> 1$ and $L/\hat{R}_0$ is order one.

Only solutions of the approximate long-wave-length model [Eqs. (35) and (36)] will now be compared with the solutions of the full system [Eqs. (11–17)]. The ELFR with small β requires large Reynolds numbers in order to obtain negative pressures along the radiatior wall $y = 0$, and hence, the lubrication model is not valid in this case. For larger β, much thinner films can be used, so that the lubrication model is applicable. We use the normal electric field as given by Eq. (43). This clearly violates the slowly varying assumptions of the derivation of the approximate models, but it will illustrate the usefulness of these models. Clearly, solving Eqs. (35) and (36) is a much easier and faster task than solving the moving

boundary problem [Eqs. (11–17)]. Hence, if the approximate models can be shown to make good predictions in the range of interest of the parameters, this justifies their usefulness.

The effect of surface tension is neglected. This should be a reasonable approximation as long as there are no regions of large curvature on the free surfaces. In a shock region (i.e., where the slope of the interface tends to infinity), surface tension is important and should not be neglected. However, our main concern is to determine how well solutions of the approximate models compare with the solutions of the full system of equations, and in particular, how well they predict the steady state. Hence, transient phenomena, unless destructive to the ELFR, are not important to us. The approximate models will be solved by using a two-step Lax-Wendroff method with diffusion and antidiffusion.[18]

Set $F = 15$ kV/cm, $\beta = 0.1$ rad, $d = 0.1$ cm, $R_0 = 6$ cm, $\Omega = 3$ rad/s, and take the other physical properties for lithium at 700 K. This gives $Re = 30.3$, $Fr = 1.0$, and $K = 45.1$. Let $H = 20\frac{1}{3}$ and $l = \frac{1}{12}$. Initial conditions are given by the steady-state shapes of the Karman-Pohlhausen method [Eqs. (35) and (36)] without the electric field. At $t = 0$, the electric field is turned on and a disturbance is generated. In Fig. 4a we plot the dimensionless film thickness h as a function of x for $t_n = n(0.01)$, $n = 0, \ldots, 6$. Here, the profile develops into a shock under the foil. We note, as in the steady-state solutions illustrated in Fig. 3, the initial depression and then rise of the surface under the charged foil. In Fig. 4b we plot the dimensionless bottom pressure as a function of time for this case at the same time steps. As noted in Sec. II, the pressure in the vacuum above the film is set to zero and the pressure below the wall is assumed to be zero for the ELFR. Hence, if a puncture were to occur directly below the foil at $x = 0$, the pressure in the fluid on the bottom of the wall and directly above the puncture should be negative in order to stop a leak. From Fig. 4b the pressure becomes negative, and therefore, this is a good operating set of parameters.

How well do the approximate models compare with the exact numerical predictions? In Fig. 4c we plot the solution of the time-dependent Karman-Pohlhausen model [Eqs. (35) and (36)]. Note the surface deformation trend is very similar to that of the exact answer, where the initial condition is the steady-state film thickness of the Karman-Pohlhausen model without an electric field. In Fig. 4d we plot the bottom pressure predicted by Eqs. (35) and (36). These compare very well. Hence, this model gives good predictions at this Reynolds number, $Re = 30.3$. For $h = 1$ and $q = 1$ at the upstream boundary, the steady-state solution of the Karman-Pohlhausen model with the electric field at $Re = 30.3$, predicted a shock under the foil. Without the electric field, as noted by the initial data shown in Fig. 4a, the height is decreasing and continuous. Hence, the effect of the electric field at this Reynolds number is to increase the height above the critical value required for a shock to occur in the Karman-Pohlhausen model, and therefore, no continuous steady state exists.

In Fig. 5, the initial d is doubled from that in Fig. 4, while the other parameters are the same. The effect of this is to raise the Reynolds number and to decrease K. Now we have $Re = 242.0$, $Fr = 2.8$, $K = 22.5$, and $H = 10$. In Figs. 5a and 5b we plot the height h and pressure, respectively, for t_n

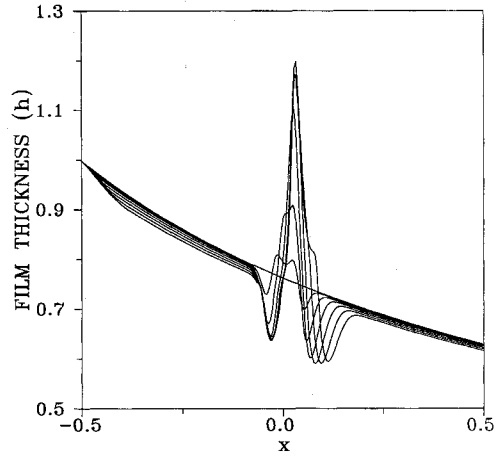

a) h vs x as determined by Eqs. (11–17)

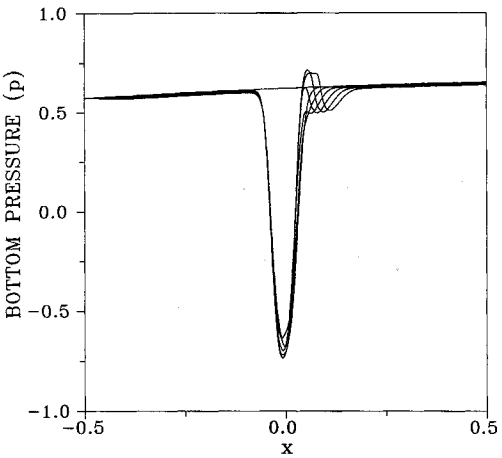

b) p vs x as determined by Eqs. (11–17)

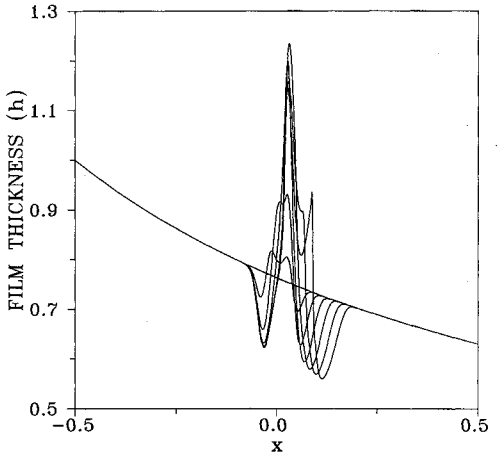

c) h vs x as determined by the Karman-Pohlhausen model [Eqs. (35) and (36)]

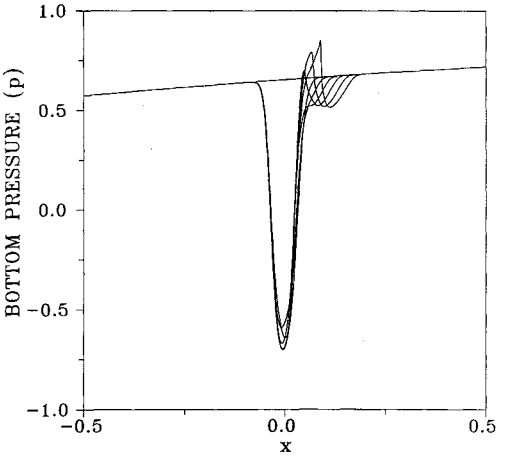

d) p vs x as determined by the Karman-Pohlhausen model [Eqs. (35) and (36)]

Fig. 4 Free surface profiles for $t = n(0.01)$, $n = 0, \ldots, 6$ with $F = 15$ kV/cm, $\beta = 0.1$ rad, $d = 0.1$ cm, $\Omega = 3$ rad/s, $\sigma = 0$, $Re = 30.3$, $K = 37.6$, $H = 20$, and the other parameter for lithium at 700 K.

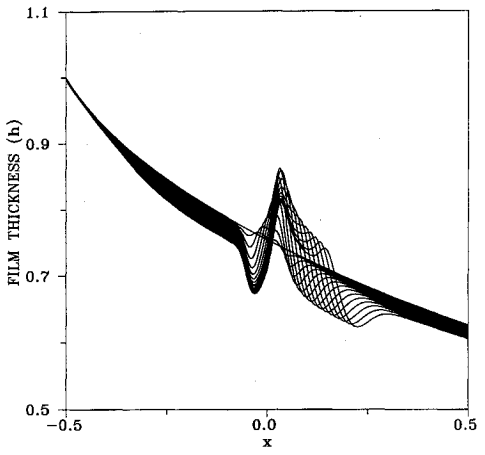

a) h vs x as determined by Eqs. (11–17)

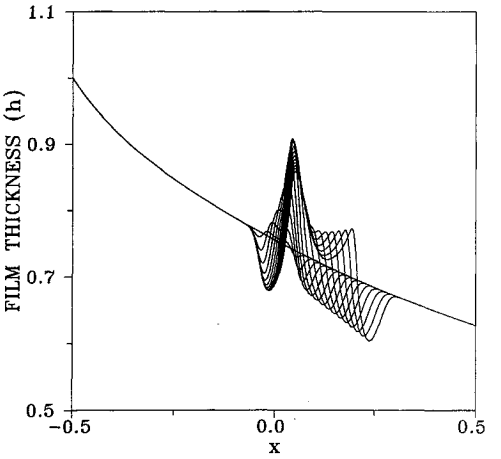

c) h vs x as determined by the Karman-Pohlhausen model [Eqs. (35) and (36)]

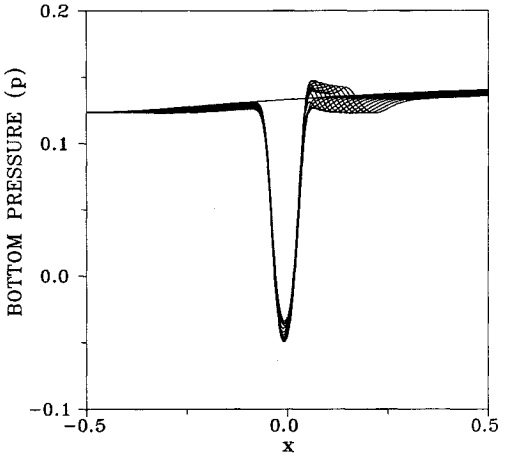

b) p vs x as determined by Eqs. (11–17)

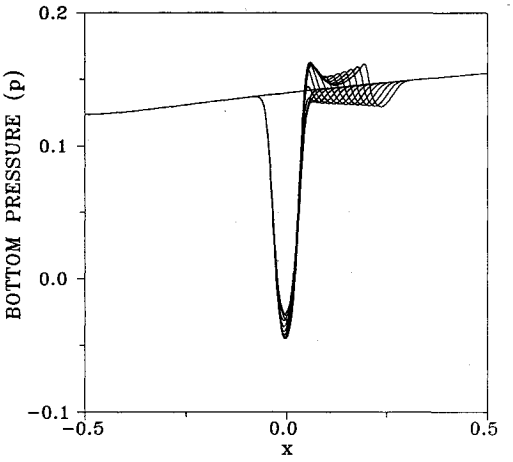

d) p vs x as determined by the Karman-Pohlhausen model [Eqs. (35) and (36)]

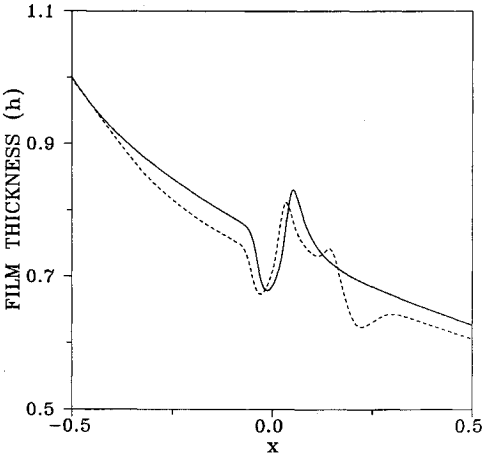

e) h vs x as determined by the steady-state Karman-Pohlhausen model (——) and the last computed time step shown in Fig. 6a (-----)

Fig. 5 Free surface profiles for $t = n(0.01)$, $n = 0, \ldots, 15$ with $F = 15$ kV/cm, $\beta = 0.1$ rad, $d = 0.2$ cm, $\Omega = 3$ rad/s, $\sigma = 0$, $Re = 242.0$, $K = 22.5$, $H = 10$, and the other parameter for lithium at 700 K.

$= n(0.01)$, $n = 0, \ldots, 15$. As in the smaller Re case of Fig. 4, the height of the film under the foil will at first decrease with increasing x and then increase. Note that the film will now rise up to about 15% of its equilibrium height. The peak height at steady state is at around $h = 0.83$, which is much smaller than the results in Fig. 4, because the increased inertial force makes the effect of the electric field weak. As time increases, a disturbance begins along the precursor trough and develops into a shock. This event is harmless since it occurs downstream of the foil and has a small amplitude. Hence, it will be washed away. In Figs. 5c and 5d we plot the results from the Karman-Pohlhausen model. There are qualitative similarities in the shape and speed of propagation of the disturbance. Also, the pressures compare very well. There are some quantitative differences. In particular, the shock occurs at an earlier time when compared to the exact numerical solution as plotted in Fig. 5a. We have only computed the time-dependent problem up to the time of formation of the shocks. Since the steady-state solution without a shock is approached, it would be enough for us to know just this

steady-state result. In Fig. 5e we plot the steady-state Karman-Pohlhausen model and the last computed time step shown in Fig. 5a. The disturbance under the foil is very close to the steady-state profile of the Karman-Pohlhausen model.

These plots illustrate that the steady-state profiles, as given by the Karman-Pohlhausen model, give good predictions at large Reynolds numbers of the true steady-state film profiles (if the profile is continuous). On the other hand, the transient profiles, although they have qualitative similarities, have quantitative differences.

VI. Conclusions

The purpose of this investigation was to study the effect of an electrostatic field on a liquid film flowing within a rotating conical radiator, and to develop model equations for the flow which will allow easy predictions of the deformation of the interface and of the pressures under the charged foil. We have shown that the presence of the electric field can change the stability of the film, and that it can, for realistic values of the parameters, produce a negative pressure under the foil, which would stop a leak out of a puncture. The Karman-Pohlhausen model has been shown to be a reliable model to predict the deformation of the interface and the pressure in the steady state. For time-dependent flows, the Karman-Pohlhausen model shows many similarities to the exact solution, but there are many quantitative differences. For the purpose of the ELFR, the steady-state result is very important, since we can expect the downstream transient behavior to be washed away with the film, and hence, have little effect on the design of the ELFR. Of course, if a second hole were to occur upstream of the first, this transient flow would affect the behavior of the film under the first foil, but again this disturbance would be washed away.

We have neglected surface tension in our study of the evolution of a disturbance along the film. Although, as noted in Fig. 2, it can have a significant effect on the stability of the film, we expect (except for regions of very large curvature, e.g., near a shock) it to have very little effect on the shape of the steady-state profiles for the liquids we are considering. On the other hand, it is expected to have a significant effect in determining at what pressures the liquid will actually leak from a puncture. The effect of surface tension will be to stop a leak because of the large additional negative capillary pressure it contributes at the puncture. Therefore, our predictions are strongly on the conservative side, since they do not include this large negative capillary pressure at the hole ($\approx 10^5$ Pa).

Acknowledgments

This work was partially supported by Department of Energy Grant DE-FG07-89FR12894. We thank C. W. Hirt, Flow Sciences, Inc., for suggesting the use of SOLA and for supplying us with a copy of the code.

References

[1]Kim, H., Bankoff, S. G., and Miksis, M. J., "Lightweight Space Radiator with Leakage Control by Internal Electrostatic Fields," *Proceedings of the Eighth Symposium on Space Nuclear Power Systems*, Albuquerque, NM, Jan. 1991, pp. 1280–1285.

[2]Rovang, R., private communication, Rocketdyne Corp., Canoga Park, CA, 1992.

[3]Bankoff, S. G., Miksis, M. J., Kim, H., and Gwinner, R., "Design Considerations for the Electrostatic Liquid-Film Radiator," Applied Mathematics TR 9135, Northwestern Univ., Evanston, IL, 1992.

[4]Kim, H., Miksis, M. J., and Bankoff, S. G., "The Electrostatic Liquid-Film Radiator for Heat Rejection in Space," *Topics in Heat Transfer*, Vol. 3, American Society for Mechanical Engineers, HTD-Vol. 206-3, New York, 1992, pp. 35–40.

[5]Kim, H., Bankoff, S. G., and Miksis, M. J., "The Effect of an Electrostatic Field on Film Flow Down an Inclined Plane," *Physics of Fluids A*, Vol. 4, No. 10, 1992, pp. 2117–2130.

[6]Landau, L. D., Lifshitz, E. M., and Pitaevskii, L. P., *Electrodynamics of Continuous Media*, 2nd ed., Pergamon, New York, 1984.

[7]Benjamin, T. B., "Wave Formation in Laminar Flow Down an Inclined Plane," *Journal of Fluid Mechanics*, Vol. 2, Aug. 1957, pp. 554–574.

[8]Yih, C. S., "Stability of Liquid Flow Down an Inclined Plane," *Physics of Fluids*, Vol. 6, No. 3, 1963, pp. 321–334.

[9]Press, W. H., Flannery, B. P., Teukolsky, S. A., and Vetterling, W. T., *Numerical Recipes, The Art of Scientific Computing*, Cambridge Univ. Press, Cambridge, England, UK, 1986, pp. 582–588.

[10]Benney, D. J., "Long Waves on Liquid Films," *Journal Mathematics and Physics*, Vol. 45, No. 2, 1966, pp. 150–155.

[11]Gjevik, B., "Occurrence of Finite-Amplitude Surface Waves on Falling Liquid Films," *Physics of Fluids*, Vol. 13, No. 8, 1970, pp. 1918–1925.

[12]Kim, H., "The Dynamics of Selected Thin-Film Flows with Internal Electrostatic Fields," Ph.D. Dissertation, Dept. of Chemical Engineering, Northwestern Univ., Evanston, IL, 1992.

[13]Prokopiou, T., Cheng, M., and Chang, H.-C., "Long Waves on Inclined Films at High Reynolds Number," *Journal of Fluid Mechanics*, Vol. 222, Jan. 1991, pp. 665–692.

[14]Rahman, M. M., Faghri, A., Hankey, W. L., and Swanson, T. D., "Heat Transfer to a Thin Liquid Film with a Free Surface," *Proceedings of the National Heat Transfer Conference*, Vol. 110, 1989, pp. 161–168.

[15]Hirt, C. W., Nichols, B. D., and Romero, N. C., "SOLA-A Numerical Solution Algorithm for Transient Fluid Flows," Los Alamos Scientific Lab. of the Univ. of California, Los Angeles, CA, 1975.

[16]Harlow, F. H., and Welch, J. E., "Numerical Calculation of Time-Dependent Viscous Incompressible Flow," *Physics of Fluids*, Vol. 8, No. 11, 1965, pp. 2182–2189.

[17]Morse, P. M., and Feshbach, H., *Methods of Theoretical Physics*, McGraw-Hill, New York, 1953.

[18]Sod, G. A., *Numerical Methods in Fluid Dynamics: Initial and Initial Boundary-Value Problems*, Cambridge Univ. Press, New York, 1985.